

Diffusion Weighted Image MRI in Assessment of Patients with Multiple Myeloma

Thesis

*Submitted for Partial Fulfilment of Master Degree in
Radio-diagnosis*

Presented by

Arwa Adel Mahmoud Hendy
M.B.B.Ch, Ain Shams University

Under supervision of

Dr. Reem Hassan Basiouny

*Assistant Professor of Radiodiology
Faculty of Medicine
Ain Shams University*

Dr. Rasha Tolba Khattab

*Lecturer of Radiodiology
Faculty of Medicine
Ain Shams University*

**Faculty of Medicine
Ain Shams University**

2018

بِسْمِ اللَّهِ الرَّحْمَنِ الرَّحِيمِ

قالوا

سببنا انك لا تعلم لنا
إلا ما علمتنا إنك أنت
العليم العظيم

صدق الله العظيم

سورة البقرة الآية: ٣٢

Acknowledgment

*First and foremost, I feel always indebted to **ALLAH**,
the Most Kind and Most Merciful.*

*I'd like to express my respectful thanks and
profound gratitude to **Dr. Reem Hassan
Basiouny**, Assistant Professor of Radiodiagnosis -
Faculty of Medicine- Ain Shams University for his
keen guidance, kind supervision, valuable advice
and continuous encouragement, which made
possible the completion of this work.*

*I am also delighted to express my deepest
gratitude and thanks to **Dr. Rasha Tolba
Khattab**, Lecturer of Radiodiagnosis, Faculty of
Medicine, Ain Shams University, for his kind care,
continuous supervision, valuable instructions,
constant help and great assistance throughout this
work.*

*I would like to express my hearty thanks to all
my family for their support till this work was
completed.*

*Last but not least my sincere thanks and
appreciation to all patients participated in this
study.*

Auwa Adel Mahmoud Hendy

List of Contents

Title	Page No.
List of Tables	i
List of Figures	ii
List of Abbreviations	v
Introduction	1
Aim of the Work.....	3
Review of Literature	
Anatomy of The Spine & bone marrow	4
MR Imaging of the Normal Bone Marrow	13
Pathology of Multiple Myeloma	22
MRI Imaging of Bone Marrow In Multiple Myeloma.....	29
Diffusion Weighted Imaging Principles	38
The Application of DWI in Multiple Myeloma.....	47
Patients and Methods	54
Results	61
Case presentation.....	68
Discussion	76
Summary	85
Conclusion.....	86
References	87
Arabic Summary	

List of Tables

Table No.	Title	Page No.
Table (1):	Comparison between the studied groups regarding ADC value.....	62
Table (2):	Comparison between the subtypes of multiple myeloma regarding ADC value	64

List of Figures

Fig. No.	Title	Page No.
Fig. (1-1):	Vertebral body.....	5
Fig. (1-2):	A: Sagittal CT MIP of the lumbar spine demonstrating the vertebral body (B), pedicle (P), superior articular process (SAP), inferior articular process (IAP), and zygapophyseal joint (Z)	5
Fig. (1-3):	Intervertebral disc	6
Fig. (1-4):	Ligaments	7
Fig. (1-5):	Sagittal T2 fat-saturated (A) and axial T2-weighted (B) MRIs of the lumbar spine demonstrating high signal intensity in the nucleus pulposus (NP) and inner annulus fibro-sis and decreased signal in the outer annulus fibrosis (AF)	8
Fig. (1-6):	Spines.....	9
Fig. (2-1):	Normal bone marrow in an 8-year-old child	15
Fig. (2-2):	Normal appearance of spinal bone marrow in a 45-year-old woman	15
Fig. (2-3):	Bone marrow conversion and re-conversion	17
Fig. (2-4):	Normal appearance of adult bone marrow on MRI	19
Fig. (2-5):	Sagittal in-phase (A) and out-of-phase (B) T1-weighted images	21
Fig. (3-1):	Normal immunoglobulin molecule containing paired heavy chains with one smaller light chain attached to each.....	23
Fig. (3-2):	Origins of plasma cells	24
Fig. (3-3):	Myeloma-induced bone defects.	26
Fig. (4-1):	Appearance of MM lesions	34
Fig. (4-2):	Bone marrow infiltration patterns	34

List of Figures (cont...)

Fig. No.	Title	Page No.
Fig. (4-3):	Sagittal T1-weighted (left) and fat-suppressed T2-weighted (right) images of the spine displaying a diffuse bone marrow infiltration of the cervical, thoracic, lumbar and sacral spine with low signal intensity on T1- and intermediate to high signal intensity on fat-suppressed T2-weighted images.....	36
Fig. (4-4):	Sagittal T1-weighted and fat-suppressed T2-weighted images of the sacrum with a new focal lesion in the vertebral body of S2, hypointense on T1- and hyperintense on T2- weighted images with a diffuse hypointense signal on a T1-weighted image of the surrounding bone marrow	36
Fig. (5-1):	Diffusion of water molecules.	39
Fig. (5-2):	a)DWI (b value = 500 sec/mm ²) shows liver metastasis (arrow), renal cyst and gallbladder all of which exhibit high signal intensity. (b) Corresponding ADC map, the metastasis shows low diffusivity reflected by the low ADC, while the cyst and gallbladder show high ADC, because of the long T2 relaxation time of the fluid (static water contents or T2 shine-through).....	42
Fig. (6-1):	Example of sequence images belongs to a patient with multiple myeloma.....	48
Fig. (6-2):	Another Example of diffusion-weighted b-value images b0, b200, b400, b600, and b1,000 in a patient with multiple myeloma	50

List of Figures (cont...)

Fig. No.	Title	Page No.
Fig. (6-3):	Diffusion-weighted b0 and b1,000 image with a region-of-interest in the vertebral body of T10 and L3 for the calculation of the apparent diffusion coefficient (ADC) in this patient with multiple myeloma and typical focal hyperintense lesions with a slightly diffusely increased signal intensity of the entire vertebral body	50
Fig. (6-4):	Diffusion-weighted b1,000 images of a patient with monoclonal gammopathy of undetermined significance demonstrating hypointense signal intensity, indicating normal fatty marrow	52
Fig. (8-1):	Pie chart demonstrating the gender of the study group	61
Fig. (8-2):	Comparison between the studied groups regarding ADC value	63
Fig. (8-3):	Comparison between the subtypes of multiple myeloma regarding ADC value	65
Fig. (8-4):	Receiver operating characteristic curve (ROC) for ADC value in differentiation between focal group and normal in focal group	66
Fig. (8-5):	Receiver operating characteristic curve (ROC) for ADC value in differentiation between diffuse group and normal MM group	67

List of Abbreviations

<i>Abb.</i>	<i>Full term</i>
<i>ADC</i>	<i>Apparent diffusion coefficient</i>
<i>DCE</i>	<i>Dynamic contrast-enhanced</i>
<i>DWI</i>	<i>Diffusion weighted imaging</i>
<i>Fs</i>	<i>Fat-suppressed / fat-saturated</i>
<i>MDCT</i>	<i>Multidetector computed tomography</i>
<i>MGUS</i>	<i>Monoclonal gammopathy of undetermined significance</i>
<i>MM</i>	<i>Multiple myeloma</i>
<i>M-protein</i>	<i>Monoclonal protein</i>
<i>MRI</i>	<i>Magnetic resonance imaging</i>
<i>SE</i>	<i>Spin-echo</i>
<i>SMM</i>	<i>Smouldering multiple myeloma</i>
<i>T1-weighted</i>	<i>T1-weighted spin-echo</i>
<i>T2-weighted</i>	<i>T2-weighted spin-echo</i>

INTRODUCTION

Multiple myeloma (MM) is a hematologic malignancy characterized by abnormal plasma cells in the bone marrow and/or in extramedullary sites, urinary and/or serum monoclonal immunoglobulin, and osteolytic lesions in most patients. The Durie and Salmon staging system for MM, which was introduced in 1975, is still used to assess tumor burden and prognosis. The plain radiographic skeletal survey is an important part of this system, since multiple osteolytic lesions define stage III disease (*Palumbo and Anderson, 2011; Rajkumar et al., 2014*).

The prognostic implications of magnetic resonance (MR) imaging of the bone marrow for MM have already been established for abnormal versus normal MR imaging results and for individual MR imaging patterns of involvement (*Song et al., 2014*) For example, abnormal spinal MR imaging results have been shown to help identify patients with asymptomatic (smoldering) myeloma who are likely to benefit from early treatment (*Moulopoulos et al., 1995*).

More recently, it was shown that patients with smoldering myeloma and more than one unequivocal focal lesion on whole-body MR images have an increased risk of developing myelomarelated symptoms and should receive treatment (*Fechtner et al., 2010; Kastritis et al., 2014*). Accordingly, the most recent International Myeloma Working

Group criteria for MM incorporate MR imaging findings in the definition of symptomatic disease (*Rajkumar et al., 2014; Dimopoulos et al., 2015*).

Diffusion-weighted imaging (DWI) with calculation of apparent diffusion coefficients (ADCs) may be used as an adjunct method to increase diagnostic confidence and to better distinguish a diffuse MR imaging pattern from a normal MR imaging pattern. So far, this technique has been applied to a relatively small number of patients with myeloma, with promising results for initial assessment and prognosis (*Messiou et al., 2011a; Padhani et al., 2013*).

AIM OF THE WORK

To evaluate the apparent diffusion coefficients (ADCs) of magnetic resonance (MR) imaging patterns in the bone marrow of patients with multiple myeloma (MM) and to determine a threshold ADC that may help distinguish a diffuse from a normal pattern with high accuracy.

Chapter 1

ANATOMY OF THE SPINE & BONE MARROW

The spine is a vital functional unit that protects the spinal cord and supports the head, thorax, abdomen, and pelvis. Together, the rigid osseous structures combined with ligaments, disks, spinal cord, and spinal nerves facilitate complex motor and sensory functions required for life, be it work or play (*Harnsberger et al., 2006*).

Vertebral Body Anatomy

Except in special circumstances, the vertebrae assume a relatively constant anatomic theme and consist of a vertebral body and a vertebral (neural) arch. The vertebral body serves as a pillar, supporting the head and trunk. The posterior margin of the bodies, along with the vertebral arches, forms the bony spinal canal, protecting the spinal cord. The neural arch is formed by paired pedicles and paired lamina. Seven processes arise from the vertebral arch: paired superior and inferior articular processes, paired transverse processes, and one spinous process. The intervertebral foramen, formed by two adjacent vertebrae, allows for passage of spinal nerves and vessels (Fig. 1-1 & 1-2).

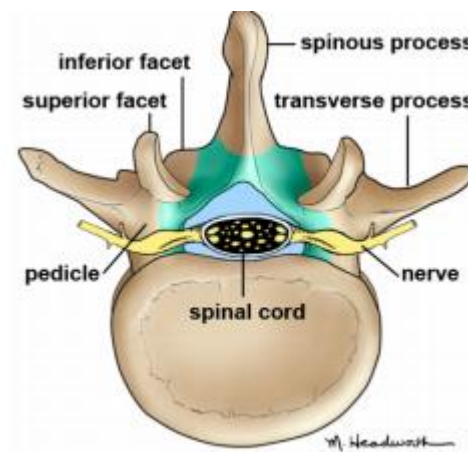


Fig. (1-1): Vertebral body.

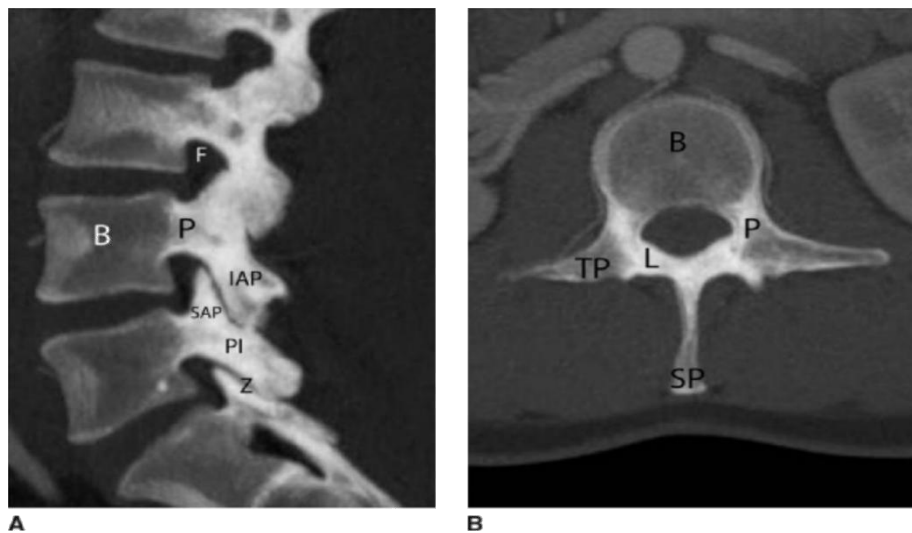


Fig. (1-2): A: Sagittal CT MIP of the lumbar spine demonstrating the vertebral body (B), pedicle (P), superior articular process (SAP), inferior articular process (IAP), and zygapophyseal joint (Z). The superior articular processes extend superiorly from the junction of the laminae and pedicles, while the inferior articular processes extend inferiorly from the undersurface of each lamina. The zygapophyseal joints are formed by the superior articular facet and the inferior articular facet. The pars interarticularis (PI) is the portion of the lamina between the superior and inferior articular processes. The intervertebral foramen (F) allows for the passage of spinal nerves and vessels. :Axial CT MIP of the lumbar spine demonstrating the vertebral body (B) and posterior neural arch. (P,pedicle; TP, transverse proocess; L, lamina; SP, spinous process).

The intervertebral discs consist of the inner nucleus pulposus and the outer annulus fibrosis. The main function of the disks is to distribute load and to allow flexion/extension and lateral bending. A remnant of the notochord, the nucleus pulposus, is usually located more dorsally compared to the center of the vertebral body. The annulus fibrosis attaches to the anterior longitudinal ligament (ALL) and posterior longitudinal ligament (PLL) and is also fused to the epiphyseal ring of the vertebral bodies. MRI of a normal disk demonstrates high signal on T2-weighted imaging related to the water content of the nucleus pulposus and inner annulus fibrosis. The outer annulus fibrosis demonstrates low signal on T1- and T2-weighted imaging (Fig 1-3) (*Harnsberger et al., 2006*).

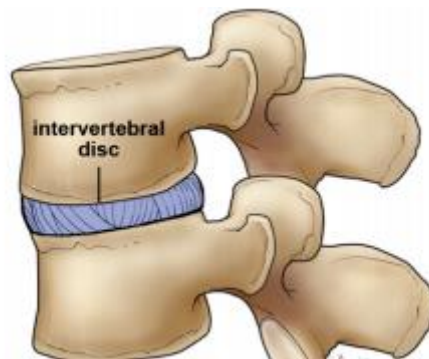


Fig. (1-3): Intervertebral disc